ISSN 2213-3437
on-line access via:
www.elsevier.com/locate/jece

JOURNAL OF ENVIRONMENTAL CHEMICAL ENGINEERING

Journal of Environmental Chemical Engineering

Aims and Scope:

The ***Journal of Environmental Chemical Engineering*** (JECE) publishes full length original research papers, short communications, review papers, perspectives and letters to the Editor. Papers are welcome which apply chemical engineering principles to understand important environmental processes or that develop/optimize novel remediation processes.

The *Journal of Environmental Chemical Engineering* provides a forum for the publication of original research on the development of alternative sustainable technologies focusing on water and wastewater treatment and reuse; treatment, reuse and disposal of waste; pollution prevention; sustainability and environmental safety; recent developments on green chemistry; alternative methods of remediation of environmental accidents including but not limited to oil spills in water bodies and nuclear accidents.

JECE calls for papers that cover the following fields:

Physico-chemical processes:
Adsorption/biosorption, ion exchange, membrane processes, magnetic separation, particle separation, phase separation, multiphase extraction, thermal/evaporative processes

Advanced oxidation processes:
Heterogeneous catalysis, UV/H_2O_2, Fenton oxidation, ozonation, sonolysis, electrochemical treatment, wet air oxidation

Nanomaterials for environmental and chemical applications:
Adsorbents, catalysts, and nanocomposites

Sustainable technologies:
Water reclamation and reuse, carbon capture, renewable energy and energy recovery, waste minimization, treatment, resource recovery

JECE also covers the following fields:
- Clean synthesis and process technology
- Source control
- Process scale-up and economic analysis
- Process integration and zero liquid discharge technologies
- Resource recovery
- Water-energy nexus
- Anthropogenic activities and environmental sustainability

Editors:

Editorial Board Members:

Processed at Thomson Digital, Gangtok (India)

Journal of Environmental Chemical Engineering 7 (2019) 103262

Contents lists available at ScienceDirect

Journal of Environmental Chemical Engineering

journal homepage: www.elsevier.com/locate/jece

Methyl violet dye removal using coal fly ash (CFA) as a dual sites adsorbent

Widi Astuti[a], Achmad Chafidz[b,*], Endang Tri Wahyuni[c], Agus Prasetya[d], I. Made Bendiyasa[d], Ahmed E. Abasaeed[e]

[a] Department of Chemical Engineering, Universitas Negeri Semarang, Semarang 50229, Indonesia
[b] Department of Chemical Engineering, Universitas Islam Indonesia, Yogyakarta 55584, Indonesia
[c] Department of Chemistry, Universitas Gadjah Mada, Yogyakarta 55281, Indonesia
[d] Department of Chemical Engineering, Universitas Gadjah Mada, Yogyakarta 55281, Indonesia
[e] Department of Chemical Engineering, King Saud University, PO Box 800, Riyadh 11421, Saudi Arabia

ARTICLE INFO

Keywords:
Adsorption
Coal fly ash
Dual sites adsorbent
Methyl violet
Isotherm model

ABSTRACT

It has become a trend to use cheap adsorbents like coal fly ash (CFA) for removal of dyes. CFA is a solid waste produced from coal-based power plant. CFA is mainly composed of minerals containing some oxides such as Al_2O_3 and SiO_2 having active sites and mesoporous unburned carbon. The existence of active sites in the CFA's minerals and carbon pores was considered to have roles in the adsorption process with different adsorption mechanisms, namely *chemisorption* for the minerals and *physisorption* for the unburned carbon. This allows the CFA to become a dual sites adsorbent. As the result, isothermal models such as Langmuir and Freundlich may not be appropriate. The objectives of this study are to develop appropriate dual sites isotherm models for methyl violet dye adsorption onto the CFA, and to compare the models with single site models including Langmuir and Freundlich. The CFAs having [Si + Al]/C ratio of 0.5, 2.0 and 90, namely CFA-1, CFA-2, and CFA-3, respectively were used in this study. X-Ray Fluorescence (XRF) analysis results showed that the major components of the original CFA are SiO_2 (36.47%) and Al_2O_3 (19.27%), while the unburned carbon content is 19.11%. Additionally, the adsorption test results showed that CFA with high unburned carbon contents (i.e. CFA-1 and CFA-2) were well fitted with the dual sites isotherm model, i.e. Freundlich–Langmuir isotherm model. Whereas, CFA with low unburned carbon contents (i.e. CFA-3) was well fitted with the single site isotherm model, i.e. Langmuir isotherm model.

1. Introduction

In recent years, colored wastewater discharged into water streams has become one of the major environmental problems. Because, it interferes with sunlight transmission into the water, and thus reduces photosynthetic process and damages the water ecosystem [1]. Dyes are also not easily degradable because of their complex aromatic structure, and are highly toxic, mutagenic and potentially carcinogenic [2,3]. Dyes can be categorized as cationic, anionic, and non-ionic [1]. Cationic dyes are considered to be even more toxic because they can pass through the entire food chain [3]. Methyl violet is an example of cationic dyes that are widely used in textile industry, paints, and paper coloring. Due to its mutagenic, carcinogenic, and mitotic poison, this dye can be considered to be harmful to living organisms as well as the ecosystem [4]. Methyl violet can also cause some health issues in human including heartbeat increase, vomiting, shock, and jaundice cyanosis, since the methyl violet can interact easily with the negatively charged membrane surface of cells, then penetrate into the cells, and deposit in the cytoplasm [2]. Therefore, it is very important to search for "*green*" processes with high efficiency and also low cost to remove methyl violet from industrial wastewater before being discharged into the water stream. Several biological and physicochemical methods have been considered to remove dyes in wastewater. These methods include aerobic [5], anaerobic [6], photocatalysis [7], coagulation [8], membrane separation [9], electrochemical treatment [10], and microwave catalysis [11]. Nevertheless, these methods have disadvantages related to high cost and production of secondary pollutants such as sludge [4].

Adsorption is one of the promising methods that has been widely studied and applied for removing dyes from industrial wastewater. The merits of adsorption include simple design, environmentally friendly, insensitivity to the toxic pollutants, ability to treat concentrated dye wastes, reusability of the spent adsorbent, high efficiency, and easy to operate [3,4,12–14]. Several organic and inorganic adsorbents have been studied by numerous reseachers, including various types of

* Corresponding author.
E-mail address: achmad.chafidz@uii.ac.id (A. Chafidz).

https://doi.org/10.1016/j.jece.2019.103262
Received 19 March 2019; Received in revised form 6 June 2019; Accepted 1 July 2019
Available online 03 July 2019

activated carbon [14–19], polymer [2], metal organic [20,21]. However, activated carbon is an expensive material although it can be regenerated [22]. Therefore, in recent years, there has been a considerable effort to find a cheaper adsorbent such as coal fly ash to remove methyl violet in wastewater [23]. Coal fly ash is a solid waste usually produced by coal-based thermal power plants. Coal fly ash mainly consists of mineral containing some oxides such as Al_2O_3 and SiO_2 that have active sites [24] and unburned carbon as a mesoporous material [25]; thus enabling coal fly ash to act as a dual-sites adsorbent.

The isotherm model is a major tool that is usually used to describe the adsorption process of a solute on the surface of adsorbent [26,27]. Most recent studies on the dye adsorption have used empirical isotherm models, such as Langmuir [28–30] and Freundlich [12,13,31–33] isotherms. However, the parameters of these models are likely not suitable for the adsorption of the dye by coal fly ash due to the existence of dual adsorption sites. Therefore, the main objectives of this research work are to prepare different coal fly ash (CFA) samples with significant different of ratio between the minerals (represented by Al_2O_3 and SiO_2) and the unburned carbon (C) as adsorbent to remove methyl violet dye via adsorption process and to find appropriate dual sites adsorption isotherm models and compare these models with single site models (e.g. Langmuir and Freundlich). To the best of our knowledge there has been no literature that specifically reported about the similar study, which make this study an interesting topic of research.

2. Material and methods

2.1. Sample preparation and characterization

Sodium hydroxide (analytical grade) was purchased from Merck. Methyl violet was purchased from CV Indrasari, Indonesia. The methyl violet contains amine group, as shown in Fig. 1. Raw coal fly ash (CFA) was obtained from a thermal power plant Tanjung Jati in Jepara, Central Java, Indonesia. Prior to any additional treatment, the raw CFA was washed using distilled water and then dried (i.e. original CFA). To study the dual site characteristic of CFA toward methyl violet dye adsorption, three CFA samples with significant different of ratio between the minerals (represented by Al_2O_3 and SiO_2) and the unburned carbon (C), i.e. [Si + Al]/C ratio of 0.5, 2.0 and 90 were used, namely CFA-1, CFA-2, and CFA-3, respectively. Each of the three samples was obtained by sieving the original CFA using 100-mesh size, reacting the original CFA with sodium hydroxide 3 M at 60 °C for 2 h, and heating the original CFA at 400 °C for 1 h, respectively. As noticed, only sample CFA-2 that underwent chemical modification, while CFA-1 and CFA-3 only underwent physical treatments. It is worth to note that these three samples were selected from our previous works [34,36].

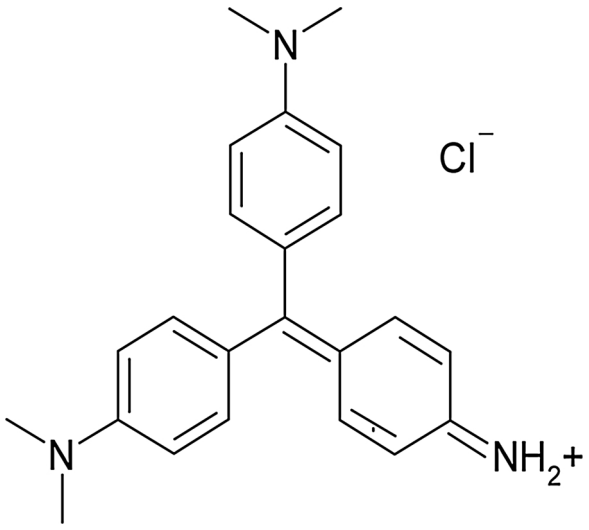

Fig. 1. Molecular structure of methyl violet dye.

Additionally, the chemical composition of original CFA was analyzed using X-Ray Fluorescence (XRF). Whereas, the crystallinity of three CFA samples was analyzed using an X-Ray Diffraction apparatus (Shimadzu XRD-6000). The total crystallinity of the CFA samples was calculated based on the number of components in the CFA that are in the crystal phase, including quartz, mullite or hydroxy sodalite. Crystallinity of quartz was calculated by comparing the intensity of two peaks of quartz in CFA with standard quartz, while crystallinity of mullite or hydroxy sodalite was determined by comparing the intensity of their three peaks in CFA with the standard of mullite or hydroxy sodalite as written in Eq. (1):

$$\text{Crystallinity} = \frac{I_A}{I_o} \times 100\% \quad (1)$$

where I_A is the intensity of quartz, mullite or hydroxy sodalite in CFA and I_o is the intensity of standard quartz, mullite or hydroxy sodalite. Additionally, Scanning Electron Microscopy (SEM) with built-in Energy-Dispersive X-ray (EDX) analysis was also performed to study the morphology and elemental analysis as well as the elemental mapping of the CFA and CFA-2. The specific surface areas of the CFA-1, CFA-2, and CFA-2 were also analyzed using an automated gas sorption apparatus with nitrogen adsorption isotherm at 77 K, and the specific surface area was determined by using a well-known Brunauer–Emmett–Teller (BET) method.

2.2. Adsorption of methyl violet dye

Batch adsorption experiments of methyl violet dye were conducted in 100 mL Erlenmeyer flasks; each flask contains 1 g of CFA sample (i.e. CFA-1, CFA-2, CFA-3) and 50 mL of methyl violet solutions with varied initial dye concentrations (i.e. 10–1000 mg L^{-1}). The adsorption experiments were carried out at pH of 9. The solution of NaOH or HCl 0.1 N was used to control the pH. The Erlenmeyer flasks containing the mixture were placed in a water bath at temperature of 26 °C and mechanically shaken at 120 rpm for 240 min. The suspended solids were then filtered using Whatman filter paper (No. 5) and the filtrates were then analyzed to determine the remaining methyl violet dye by using a UV–Vis spectrometer at λ_{max} of 581 nm. The adsorption effectivity was defined as the amount of methyl violet dye adsorbed by the CFA sample per unit mass of the CFA sample, which was expressed by Eq. (2) [26]:

$$C_\mu = \frac{(C_i - C_e)V}{m} \quad (2)$$

where C_i is the initial concentration of methyl violet (mmol L^{-1}), C_e is the concentration of methyl violet in solution at equilibrium (mmol L^{-1}), C_μ is the concentration of methyl violet on the adsorbent surface at equilibrium (mmol g^{-1}), V is the volume of methyl violet solution (L) and m is the adsorbent mass (g). To further study the adsorption mechanism of methyl violet dye, the desorption analysis was also conducted using the following procedure. The adsorbent fully loaded with the methyl violet dye was filtered using Whatman filter paper (No. 5) and then dried. Afterward, 1 g of the dried adsorbent was put into 50 mL of distilled water and stirred at 120 rpm for 240 min. The concentration of methyl violet in solution was determined using a UV–Vis spectrometer at λ_{max} of 581 nm.

2.3. Adsorption isotherm models

To study the adsorption mechanism of methyl violet onto CFA adsorbent, six isotherm models were investigated, i.e. (1) single site Langmuir, (2) single site Freundlich, (3) dual sites Langmuir–Langmuir, (4) dual sites Freundlich–Freundlich, (5) dual sites Langmuir–Freundlich, and (6) dual sites Freundlich–Langmuir. The schematic diagrams of these models are depicted in Fig. 2.

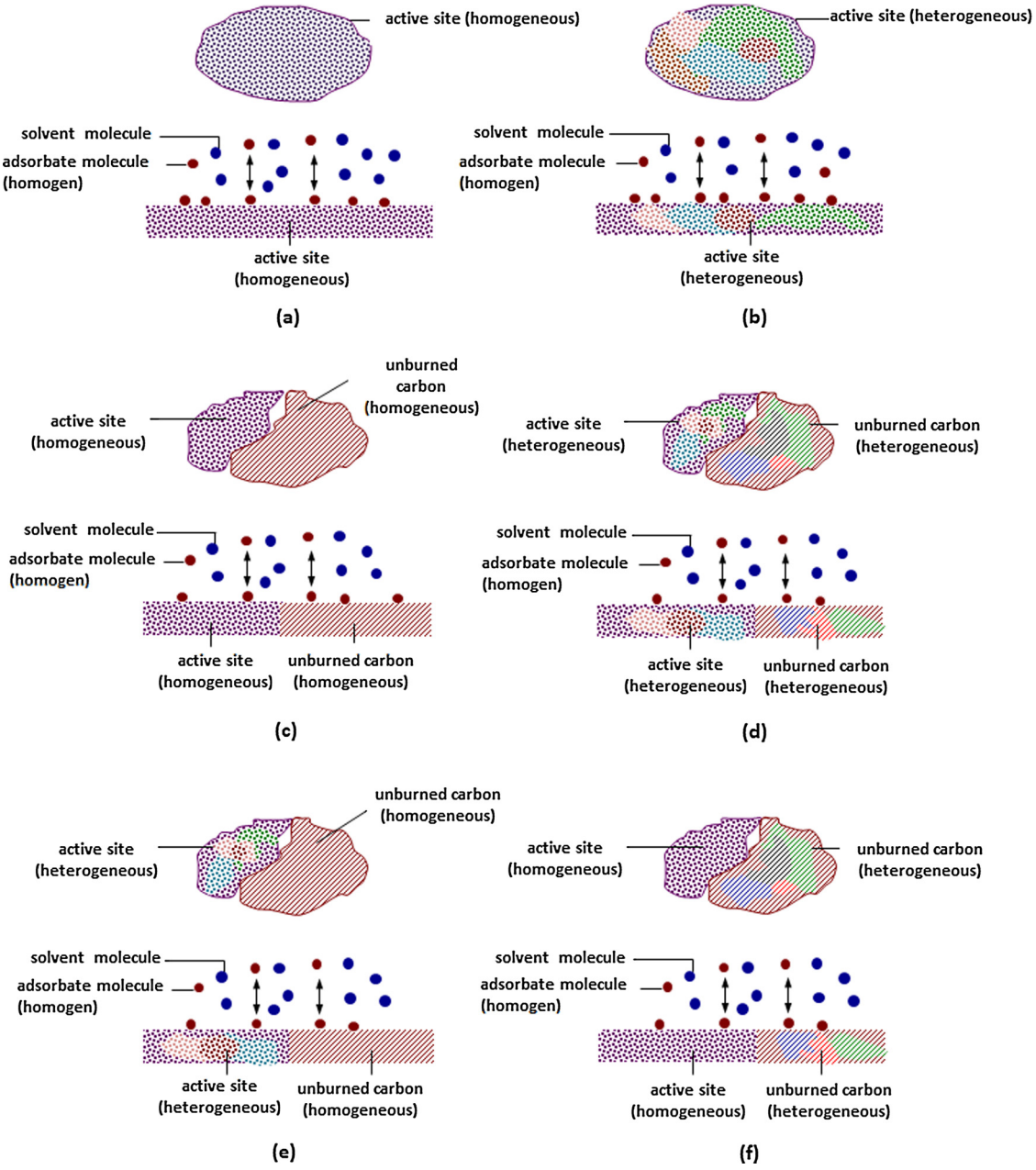

Fig. 2. Schematic diagram of adsorption for (a) model 1; (b) model 2; (c) model 3; (d) model 4; (e) model 5; and (f) model 6.

2.3.1. Model 1: single site Langmuir

In this model, the contribution of unburned carbon in the methyl violet adsorption is considered to be very small, and thus can be neglected. The adsorption process occurs on the active sites that have homogeneous energy by electrostatic interaction and is also assumed to be a localized adsorption. Therefore, once a single molecule of dye occupies a single site, no further adsorption of other dye molecules can take place on that particular site [1]. Additionally, the interaction between the adsorbate molecules is neglected. The Langmuir isotherm model is described in Eq. (3) [35]:

$$C_{\mu} = C_{\mu m}\frac{K_L C_e}{1 + K_L C_e} \tag{3}$$

where $C_{\mu m}$ is the amount of methyl violet needed to form a monolayer on unit mass of adsorbent (mmol g^{-1}) and K_L is a constant or parameter related to the affinity of the binding site (L $mmol^{-1}$) [27]. Eq. (3) was solved by optimizing the correlation coefficient between the predicted C_{μ} from Eq. (3) and the experimental data. The solver add-in feature of Microsoft Excel software can be used to determine $C_{\mu m}$ and K_L by minimizing the difference between model predicted data with the experimental data [1].

2.3.2. Model 2: single site Freundlich

This model is derived based on heterogeneous surface of mineral in CFA with a random distribution of adsorption heat over the surface [1]. The role of unburned carbon in the adsorption process is very small, thus it can be neglected. The Freundlich isotherm is expressed by Eq. (4):

$$C_{\mu} = K_F C_e^n \tag{4}$$

where K_F and n are the Freundlich parameters and also characteristics of the system. K_F ($mmol^{1-1/n} L^{1/n} g^{-1}$) is indicating the adsorption capacity, while n is indicating the adsorption intensity. The K_F and n values are determined by optimizing the correlation coefficient between the predicted C_{μ} data from the Eq. (4) and the experimental data.

Table 1
Si, Al and C content of three CFA samples.

[Si + Al]/C ratio	Components	Percentage (wt%)
0.5	Si	15.88
	Al	7.02
	C	46.15
2.0	Si	19.92
	Al	11.77
	C	16.44
90	Si	24.82
	Al	11.93
	C	0.42

The parameters K_F and n are determined by minimizing the squared difference between model predictions and experimental data [1].

2.3.3. Model 3: dual sites Langmuir–Langmuir

In this model, the unburned carbon and active sites play simultaneous roles in the adsorption process. The unburned carbon and active sites are assumed as different patches, which have different level of energies. Each patch acts independently and there is no interaction between the different patches. For the same patch, adsorption sites have homogeneous energy distribution. Energy distribution of patches on the solid surface is assumed to follow multi-modal distribution function. The adsorbate molecules are adsorbed by one site only and zero interaction between the adsorbate molecules. This model is defined by Eq. (5), as follows:

$$C_\mu = C_{\mu m1}\frac{K_{L1}C_e}{1 + K_{L1}C_e} + C_{\mu m2}\frac{K_{L2}C_e}{1 + K_{L2}C_e} \tag{5}$$

where '1' represents the unburned carbon (site 1) and '2' represents the active sites (site 2). The parameters in Eq. (5) were determined by optimizing the correlation coefficient between the C_μ predicted from Eq. (5) and experimental data.

2.3.4. Model 4: dual sites Freundlich–Freundlich

This model assumes that the unburned carbon and active sites both are contributing to the adsorption process. Similar to the previous model, both unburned carbon and active sites are also considered as different patches, which have different level of energies. The model is given by Eq. (6).

$$C_\mu = K_{F1}\cdot C_e^{n1} + K_{F2}\cdot C_e^{n2} \tag{6}$$

2.3.5. Model 5: dual sites Langmuir–Freundlich

Langmuir–Freundlich dual site model is expressed by Eq. (7):

$$C_\mu = C_{\mu m1}\frac{K_{L1}C_e}{1 + K_{L1}C_e} + K_{F2}\cdot C_e^{n2} \tag{7}$$

where '1' represents the adsorption on unburned carbon following Langmuir isotherm and '2' represents the adsorption on active sites following Freundlich isotherm. A trial and error procedure was done to solve Eq. (7) and to determine K_{L1}, $C_{\mu m1}$, K_{F2}, and n_2.

2.3.6. Model 6: dual sites Freundlich–Langmuir

Freundlich–Langmuir dual sites model is given by Eq. (8) as follows:

$$C_\mu = K_{F1}\cdot C_e^{n1} + C_{\mu m2}\frac{K_{L2}C_e}{1 + K_{L2}C_e} \tag{8}$$

where '1' represents the adsorption on unburned carbon following Freundlich isotherm and '2' represents the adsorption on active sites following Langmuir isotherm.

2.4. Error estimation

In this work, the sum of the square of the errors (SSE) deviation [1] was used to estimate the fitting accuracy of the studied isotherm models. The SSE deviation is given by Eq. (9).

$$SSE = \sum_{i=1}^{n}(C_{\mu,calc} - C_{\mu,meas})_i^2 \tag{9}$$

3. Results and discussion

3.1. Characteristics of the coal fly ash (CFA)

Based on our previous works, the X-Ray Fluorescence (XRF) analysis results showed that the major components of raw coal fly ash are silica, SiO_2 (36.47%) and alumina, Al_2O_3 (19.27%), while the unburned carbon content is 19.11% [34,36]. Whereas, Table 1 shows Si, Al and C content analysis results of CFA samples with [Si + Al]/C ratio of 0.5, 2.0, and 90.

Additionally, the morphology of the CFA was also observed by using a Scanning Electron Microscopy (SEM). A SEM micrograph of the original CFA is depicted in Fig. 3a. As seen in the figure, the original CFA is composed of minerals and unburned carbon, hence enable it to act as a dual sites adsorbent. As observed in the figure, the mineral has a spherical microscopic structure with a smooth surface, whereas the unburned carbon has a rougher surface with many pores. Fig. 3b shows the SEM micrograph of the CFA-2. As seen in the figure, chemical modification of the original CFA with sodium hydroxide has resulted in rougher surfaces and more holes.

Additionally, the original CFA and CFA-2 were further analyzed by using SEM-EDX. Figs. 4 and 5 show the SEM micrograph and SEM-EDX elemental mapping of original CFA and CFA-2, respectively. As observed in Figs. 4 and 5, the O, C, Al, and Si elements seemed to be well distributed on the coal fly ash surface.

To confirm the presence of alumina and silica, the three CFA

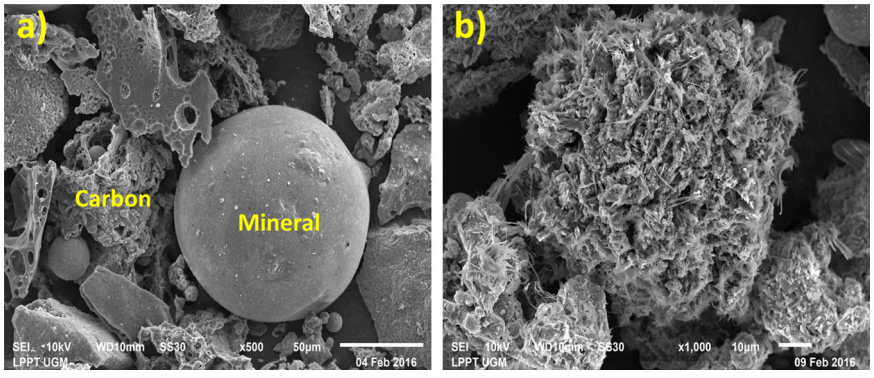

Fig. 3. SEM micrograph of (a) original coal fly ash (CFA), and (b) CFA-2 with [Si + Al]/C ratio of 2.0.

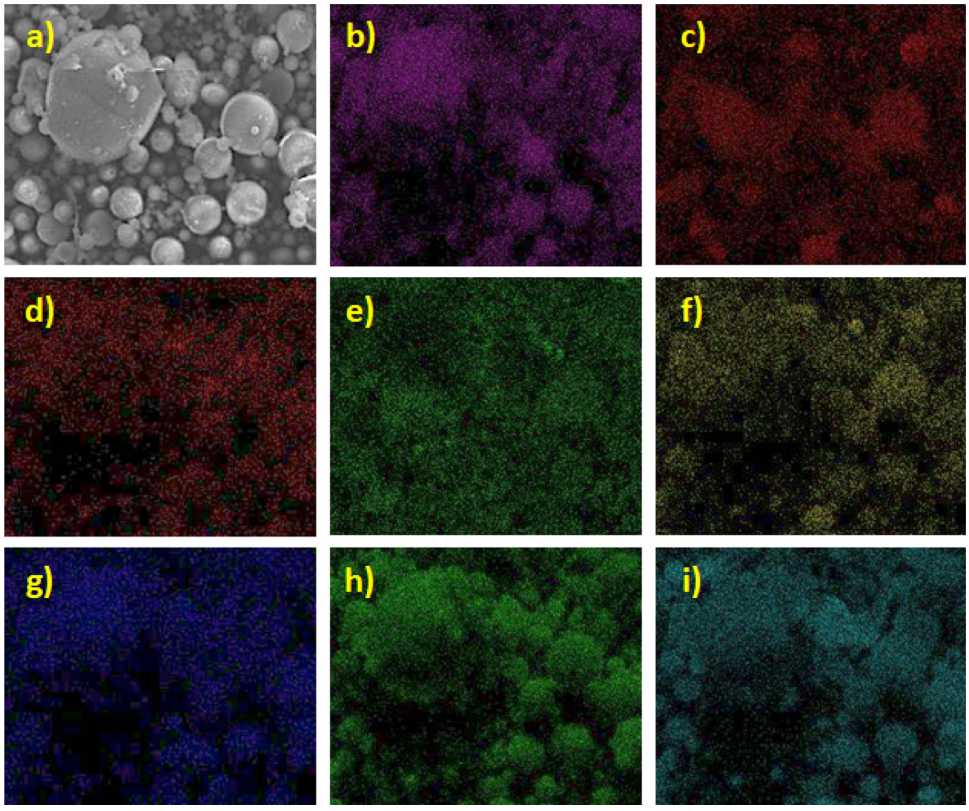

Fig. 4. (a) SEM micrograph of original CFA and SEM–EDX elemental mapping images of (b) Al content; (c) Ca content; (d) C content; (e) Fe content; (f) Mg content; (g) Na content; (h) O content; and (i) Si content (at magnification of 2000×).

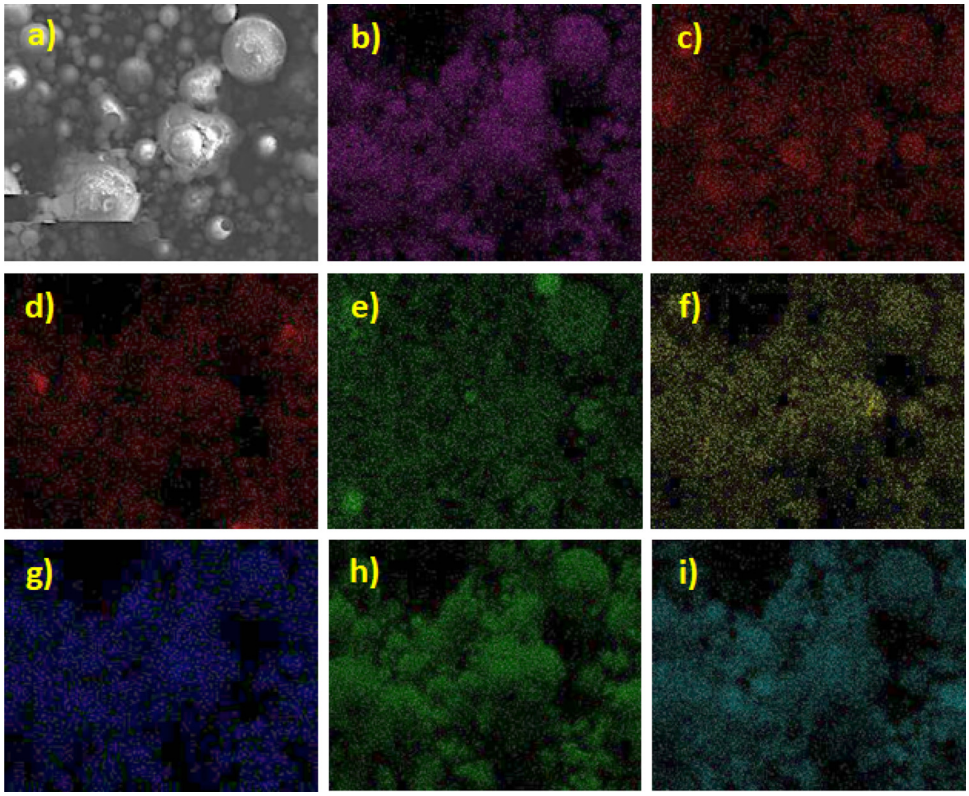

Fig. 5. (a) SEM micrograph of the CFA-2 with [Si + Al]/C ratio of 2.0 and SEM–EDX elemental mapping images of (b) Al content; (c) Ca content; (d) C content; (e) Fe content; (f) Mg content; (g) Na content; (h) O content; and (i) Si content (at magnification of 2000×).

Table 2
XRD and BET analysis results of three CFA samples.

Samples	Ratio of [Si + Al]/C	Analysis items	Values
CFA-1	0.5	Crystallinity (%)	100.0
		Specific surface area (m^2/g)	15.7
CFA-2	2.0	Crystallinity (%)	65.0
		Specific surface area (m^2/g)	80.3
CFA-3	90	Crystallinity (%)	88.2
		Specific surface area (m^2/g)	9.7

samples were further characterized using X-Ray Diffraction (XRD) apparatus. The XRD analysis results showed that the three CFA samples contained crystalline phases such as mullite ($3Al_2O_3{\cdot}2SiO_2$), quartz (SiO_2) and also other amorphous components. The total crystallinity of CFA samples with [Si + Al]/C ratio of 0.5, 2.0, and 9.0 are listed in Table 2. Additionally, BET analysis was also conducted to measure the specific surface area of the CFA samples. The results of BET analysis for three CFA samples are also listed in Table 2. As shown in the table, the total crystallinity of the CFA with [Si + Al]/C ratio of 0.5 (i.e. CFA-1) was about 100% then decreased to 88.2% and 65.0% for CFA with [Si + Al]/C ratio of 90 (i.e. CFA-3) and 2.0 (i.e CFA-2), respectively. As seen in the table, the CFA-2 has the lowest total crystallinity, but it has the highest specific surface area. This low crystallinity value indicates that amorphous phase was formed by partial damage of mullite and quartz after chemical modification of the raw CFA with sodium hydroxide, which resulted in rougher surfaces and more holes (see Fig. 3b). However, the reaction with sodium hydroxide also formed hydroxy sodalite. The higher the sodium hydroxide concentration the more hydroxyl sodalites were formed, as reported in our previous work [36].

Additionally, Fig. 6 shows the N_2 adsorption–desorption profiles of original CFA and CFA-2 with [Si + Al]/C ratio of 2.0. According to Brunauer's classification, Fig. 6a belongs to the Type III isotherm, which indicates that the adsorbent–adsorbate interaction is weak. While Fig. 6b belongs to the Type II isotherm with hysteresis loop suggesting that the CFA-2 with [Si + Al]/C ratio of 2.0 has mesopores other than macropores.

3.2. Adsorption of methyl violet

Batch adsorption experiments of methyl violet dye were carried out in this work. Fig. 7 depicts the plot of adsorption capacity (C_μ) versus initial dye concentration (C_i) during the adsorption of methyl violet by three samples of CFA (i.e. [Si + Al]/C ratio of 0.5, 2.0, and 9.0). As seen in the figure, the adsorption capacity increased with the increasing concentration of methyl violet, but then remained constant once the equilibrium point was reached. Higher initial concentration of methyl violet dye enhanced the adsorption process. As seen in Fig. 7, the CFA-1 sample with the highest unburned carbon content (i.e. [Si + Al]/C ratio ≈ 0.5) had the lowest adsorption capacity. Though unburned carbon is a mesoporous material that could contribute to the adsorption process, the role of the active sites in the oxides part of CFA was more pronounced due to its polarity. Additionally, as seen in Fig. 8, a great amount of unburned carbon formed aggregates that covered up the active sites on the mineral surface of the CFA, hence chemical bonding between the active sites and methyl violet was hindered. As the result, the amount of adsorbed methyl violet decreased with the presence of high content of unburned carbon (see Fig. 7). Additionally, the sorption mechanism of the methyl violet in the active sites refers to the following reactions [37].

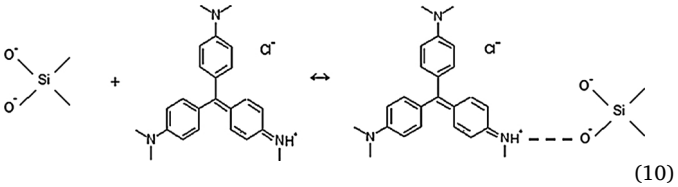

(10)

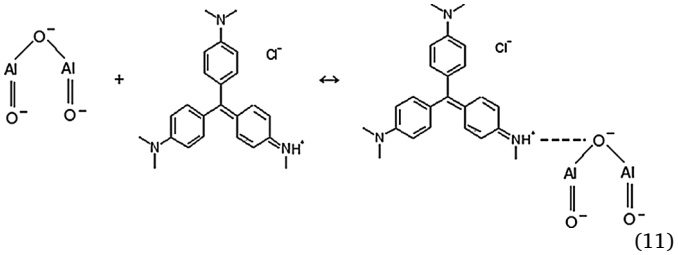

(11)

Additionally, the CFA-2 with [Si + Al]/C ratio ≈ 2.0 had the highest adsorption capacity even though the carbon content was higher than that of the CFA-3 with [Si + Al]/C ratio ≈ 90. It is because the reaction of CFA with NaOH may decrease the crystallinity of quartz and mullite; hence the active sites become more open, hence more accessible to the methyl violet molecules. This confirms further that active sites play a larger role in adsorption than the carbon. Additionally, to further study the adsorption characteristics of the CFA, desorption experiments on the used CFA samples were carried out; the results for CFA-1 and CFA-3 with [Si + Al]/C ratio ≈ 0.5 and 90, respectively are presented in Table 3. The CFA samples that have been used to adsorb methyl violet dye were agitated in distilled water to desorb the methyl violet dye. If methyl violet dye can be easily desorbed by distilled water indicates that the adsorption force is weak. As seen in Table 3, only 1–3% of methyl violet could be desorbed by distilled water. This indicates that adsorption force and the chemical binding interactions were quite strong since the most of the adsorption occurred at the active sites.

3.3. Adsorption isotherm models

Freundlich and Langmuir isotherm models are usually used to describe the adsorption process of dyes. However, the presence of carbon

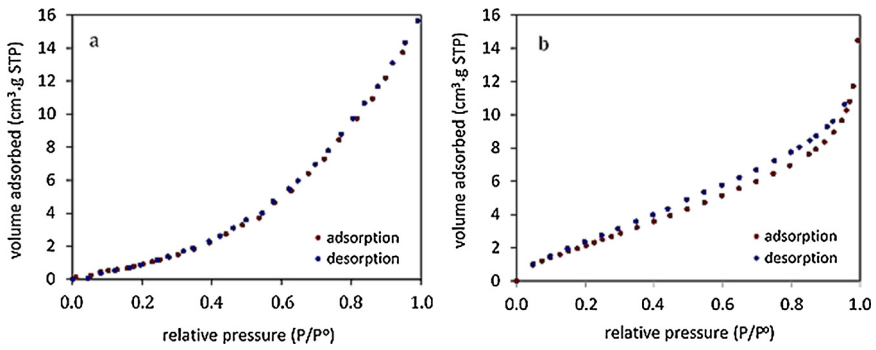

Fig. 6. The adsorption–desorption isotherms of N_2 at 77 K for (a) original CFA and (b) CFA-2 with [Si + Al]/C ratio of 2.0.

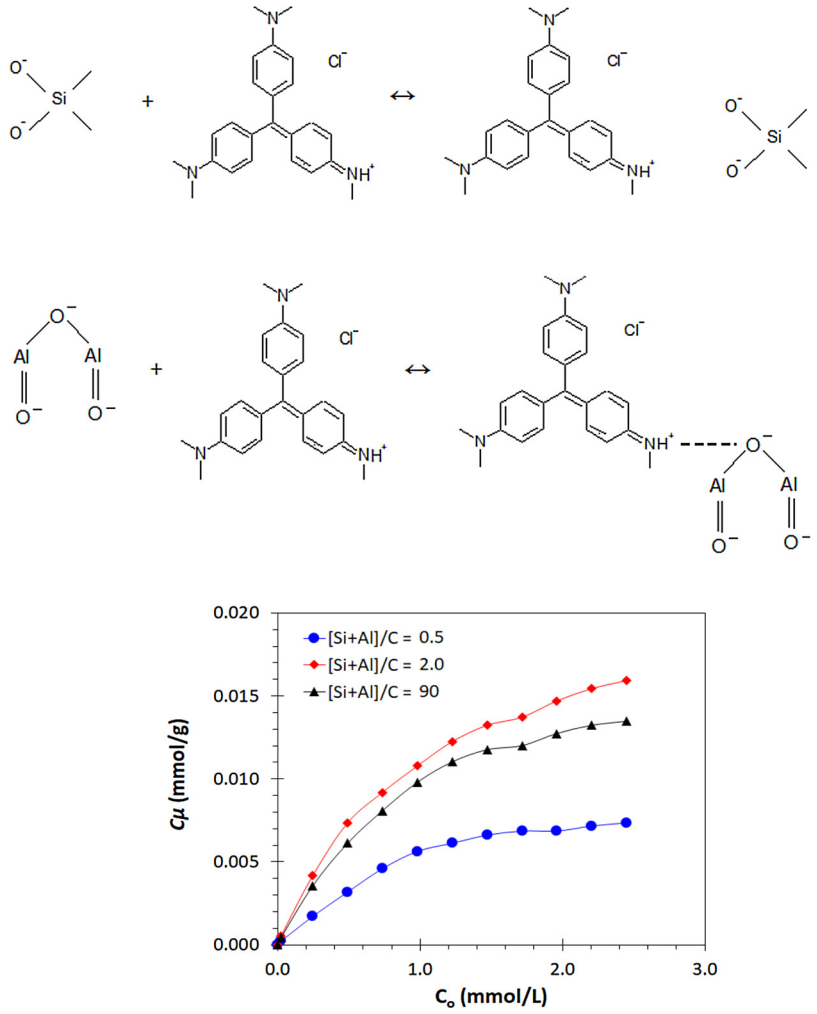

Fig. 7. Adsorption of methyl violet by three samples of CFA (CFA = 1 g per 50 mL of methyl violet dye solution, contact time = 240 min, and pH = 9).

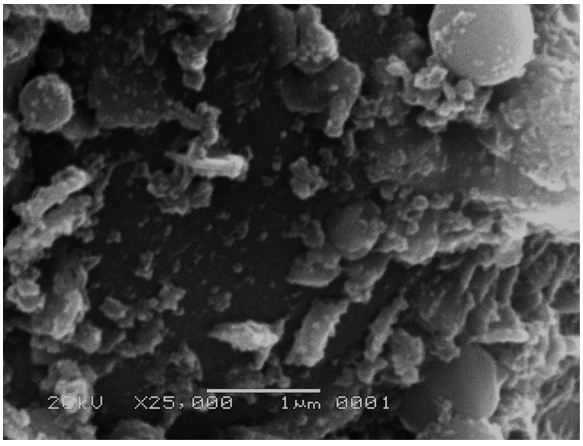

Fig. 8. SEM micrograph of mineral surface of the CFA-1 with [Si + Al]/C ratio of 0.5 which covered by the unburned carbon (at magnification of 25,000×).

and minerals in the coal fly ash (CFA) renders these models inappropriate. In this work, single site isotherm models such as Freundlich and Langmuir were compared to the dual sites isotherm models including Langmuir–Langmuir, Freundlich–Freundlich, Langmuir–Freundlich, and Freundlich–Langmuir. Values of sum squared errors (SSE) of isotherm model are presented in Table 4, while the average deviation of the predicted C_μ versus C_μ experimental data are described in Table 5. The two tables show that Freundlich–Langmuir model was in accordance with experimental data for CFA samples with [Si + Al]/C ratio of 0.5 (i.e. CFA-1) and 2.0 (i.e. CFA-2), since they have smallest SSE and average deviation. There were enough carbons in the CFA samples and active sites on SiO_2–Al_2O_3 surface of the CFA samples that could contribute into the methyl violet dye adsorption. Therefore, the dual sites model was more appropriate to be used than the single site model. On other hand, for CFA-3 with [Si + Al]/C ratio 90, Langmuir isotherm as a single site model was in accordance with experimental data. It was because the carbon content of the ash was very small, so that it was not enough to contribute to the adsorption process of methyl violet dye. Table 6 shows the isotherm

Table 3
The amount of methyl violet adsorbed and desorbed by CFA-1 and CFA-3.

Items	[Si + Al]/C ≈ 90 (i.e. CFA-3)	[Si + Al]/C ≈ 0.5 (i.e. CFA-1)
Methyl violet adsorbed, mmol g^{-1}	0.0147	0.0103
Methyl violet desorbed, mmol g^{-1}	0.0003	0.0003
Methyl violet desorbed, %	1.83	3.12

Table 4
Values of SSE error analysis of isotherm model of dye on three CFA samples.

No.	Isotherm models	SSE for CFA samples with ratio of:		
		[Si + Al]/C ≈ 0.5 (i.e. CFA-1)	[Si + Al]/C ≈ 2.0 (i.e. CFA-2)	[Si + Al]/C ≈ 90 (i.e. CFA-3)
1	Langmuir	3.09×10^{-6}	6.83×10^{-5}	5.22×10^{-6}
2	Freundlich	2.30×10^{-4}	3.97×10^{-3}	7.13×10^{-4}
3	Langmuir–Langmuir	2.42×10^{-6}	1.93×10^{-5}	7.33×10^{-5}
4	Freundlich–Freundlich	2.82×10^{-5}	1.57×10^{-3}	4.90×10^{-5}
5	Langmuir–Freundlich	9.58×10^{-6}	1.26×10^{-4}	2.74×10^{-5}
6	Freundlich–Langmuir	1.47×10^{-6}	1.86×10^{-5}	3.86×10^{-5}

Table 5
Average deviation of C_μ predicted data toward C_μ experimental data.

No.	Isotherm models	Average % deviation of predicted C_μ from experimental C_μ for CFA samples with ratio of:		
		[Si + Al]/C ≈ 0.5 (i.e. CFA-1)	[Si + Al]/C ≈ 2.0 (i.e. CFA-2)	[Si + Al]/C ≈ 90 (i.e. CFA-3)
1	Langmuir	14.0	13.2	6.3
2	Freundlich	53.6	30.5	43.4
3	Langmuir–Langmuir	7.8	9.7	22.3
4	Freundlich–Freundlich	17.6	17.9	22.5
5	Langmuir–Freundlich	17.6	17.9	22.3
6	Freundlich–Langmuir	4.6	8.2	16.8

Table 6
The isotherm parameters for adsorption of methyl violet onto three CFA samples.

Parameters	CFA samples with ratio of:		
	[Si + Al]/C ≈ 90 (i.e. CFA-3) (based on model 1)	[Si + Al]/C ≈ 2.0 (i.e. CFA-2) (based on model 6)	[Si + Al]/C ≈ 0.5 (i.e. CFA-1) (based on model 6)
$C_{\mu m}$	0.0183	–	–
K_L	2.3716	–	–
K_{F1}	–	0.0011	0.0063
n_1	–	2.0362	1.8768
$C_{\mu m2}$	–	0.0541	0.0099
K_{L2}	–	2.9014	1.0082

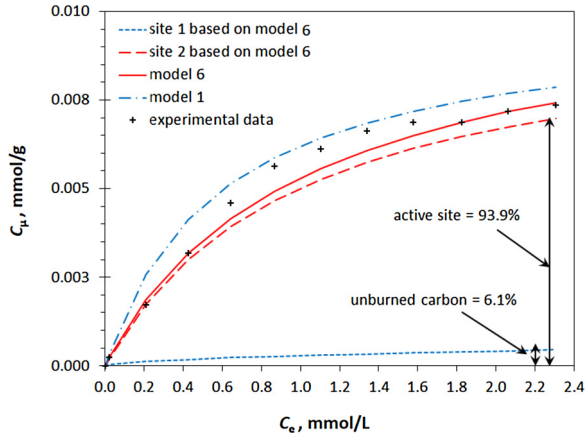

Fig. 9. Comparison between methyl violet dye adsorbed on the active sites and the unburned carbon based on model 1 (single site) and model 6 (dual sites) for CFA-1 with [Si + Al]/C ratio of 0.5.

parameters for the adsorption process of methyl violet onto three CFA samples.

Furthermore, the amount of methyl violet dye adsorbed on the active sites and the unburned carbon were analyzed and compared. Fig. 9 shows the amount of methyl violet dye adsorbed in the active sites and unburned carbon based on Freundlich–Langmuir isotherm (model No. 6) and Langmuir isotherm (model No. 1) for CFA-1 with [Si + Al]/C ratio of 0.5. As seen in the figure, in case of adsorption process using CFA-1 with [Si + Al]/C ratio of 0.5, the isotherm model 6 was more suitable than the isotherm model 1. Additionally, based on the result of model 6, the amount of methyl violet dye adsorbed on the active sites was higher than that of adsorbed on the unburned carbon. This indicates that the adsorption of methyl violet dye onto the surface of CFA-1 with [Si + Al]/C ratio of 0.5 mostly occured in the active sites.

On the other hand, in the adsorption process using CFA-3 with [Si + Al]/C ratio of 90 (see Fig. 10), the isotherm model 1 was more appropriate than the isotherm model 6. As seen in Fig. 10, according to the model 1 result, almost all of the methyl violet dyes were adsorbed on the active sites (i.e. 98.8%). This indicates that the CFA-3 with [Si + Al]/C ratio of 90 could not act as dual sites adsorbent due to low unburned carbon content. Additionally, the suitability of the experimental data to the single site or dual sites isotherm model is influenced by the ratio of [Si + Al]/C in the CFA samples. Fig. 11 shows the plot of average deviation of C_μ predicted data toward C_μ experimental data (%) versus the ratio of [Si + Al]/C in the CFA. As seen in the figure, the transition of model 1 (single site) to model 6 (dual sites), which was indicated by the crossing lines of both model 1 and model 6, occurred in

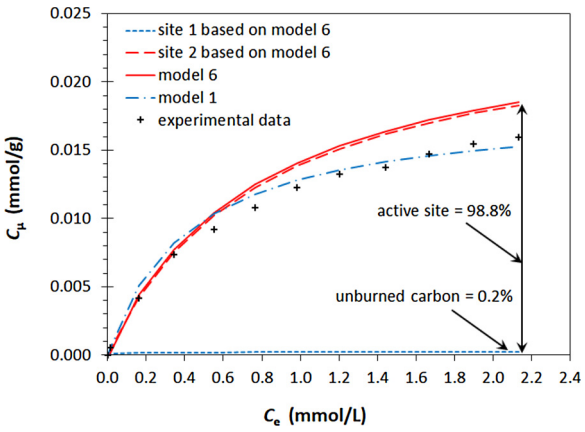

Fig. 10. Comparison between methyl violet dye adsorbed on the active sites and the unburned carbon based on model 1 (single site) and model 6 (dual sites) for CFA-3 with [Si + Al]/C ratio of 90.

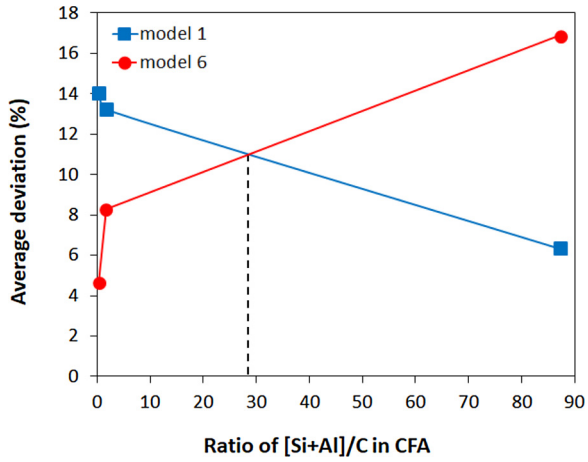

Fig. 11. The transition of isothermal model 1 (i.e. single site) to isothermal model 6 (i.e. dual sites) based on the ratio of [Si + Al]/C in CFA.

the ratio [Si + Al]/C of 27.

4. Conclusion

The coal fly ash (CFA) based adsorbent has been successfully prepared from the waste of a local coal-based power plant. To study dual site characteristic of CFA toward methyl violet dye adsorption, three CFA samples with significant different of ratio between the minerals (represented by Al_2O_3 and SiO_2) and the unburned carbon (C), i.e. [Si + Al]/C ratio of 0.5, 2.0 and 90 were prepared, namely CFA-1, CFA-2, and CFA-3, respectively. The result of morphological analysis using Scanning Electron Microscopy (SEM) showed that the CFA is mainly composed of mineral and unburned carbon, and thus enable it to act as a dual sites adsorbent. Additionally, the CFA samples were characterized by X-Ray Diffraction (XRD) and Brunauer–Emmett–Teller (BET) analysis to study the total crystallinity and specific surface area of the CFA samples, respectively. The XRD and BET analyses results showed that the CFA-2 with [Si + Al]/C ratio of 2.0 has the lowest total crystallinity, but it has the highest specific surface area. Additionally, experimental batch adsorption of methyl violet dye onto three types of CFAs were also conducted to study the adsorption mechanism and to find an appropriate isotherm model. From the batch adsorption test results, it was found that the CFA samples with relatively high carbon content (i.e. [Si + Al]/C ≈ 0.5 and 2.0), the unburned carbon part acted as a mesoporous material, which could contribute in the adsorption of methyl violet dye together with the active sites on the mineral part. Therefore, dual sites isotherm model was more appropriate for these two CFA samples (i.e. [Si + Al]/C ≈ 0.5 and 2.0) than single site isotherm model. Among four dual sites models that have been considered in this work, the Freundlich–Langmuir isotherm model (i.e. model No. 6) was seen to be well fitted (suitable) with the experimental data, as compared to other three dual sites models. Whereas, for the CFA sample with relatively low carbon content (i.e. [Si + Al]/C ≈ 90), the Langmuir isotherm model (i.e. Model No. 1) was seen to be in accordance with the experimental data. Nevertheless, the unburned carbon could plug the active sites wherein the adsorption process was mostly occurred. Hence, the existence of unburned carbon on the CFA could decrease the amount of methyl violet adsorbed.

Conflict of interest

None.

Acknowledgements

The authors would like to express their gratitude to the Ministry of Research, Technology and Higher Education of Republic Indonesia for the financial support under “Hibah Bersaing” Research Grant year 2014 with a contract number of 1.5.5/UN37/PPK.3.1/2014.

References

[1] X. Wang, C. Jiang, B. Hou, Y. Wang, C. Hao, J. Wu, Carbon composite lignin-based adsorbents for the adsorption of dyes, Chemosphere 206 (2018) 587–596.
[2] J. Liu, N. Wang, H. Zhang, J. Baeyens, Adsorption of Congo red dye on $Fe_xCo_{3-x}O_4$ nanoparticles, J. Environ. Manag. 238 (2019) 473–483.
[3] P. Rai, R.K. Gautam, S. Banerjee, V. Rawat, M.C. Chattopadhyaya, Synthesis and characterization of a novel $SnFe_2O_4$ activated carbon magnetic nanocomposite and its effectiveness in the removal of crystal violet from aqueous solution, J. Environ. Chem. Eng. 3 (2015) 2281–2291.
[4] B.C.S. Ferreira, F.S. Teodoro, A.B. Mageste, L.F. Gie, R.P. de Freitas, L.V.A. Gurgel, Application of a new carboxylate-functionalized sugarcane bagasse for adsorptive removal of crystal violet from aqueous solution: kinetic, equilibrium and thermodynamic studies, Ind. Crops Prod. 65 (2015) 521–534.
[5] L. Tan, M. He, L. Song, X. Fu, S. Shi, Aerobic decolorization, degradation and detoxification of azo dyes by a newly isolated salt tolerant yeast *Scheffersomyces spartinae* TLHS-SF1, Bioresour. Technol. 203 (2016) 287–294.
[6] W. Liu, L. Liu, C. Lieu, Y. Hao, H. Yang, B. Yuan, J. Jiang, Methylene blue enhances the anaerobic decolorization and detoxication of azo dye by *Shewanella onediensis* MR-1, Biochem. Eng. 110 (2016) 115–124.
[7] X. Zhang, Y. Wang, F. Hou, H. Li, Y. Yang, X. Zhang, Y. Yang, Y. Wang, Effects of Ag loading on structural and photocatalytic properties of flower-like ZnO microspheres, Appl. Surf. Sci. 391 (B) (2017) 476–483.
[8] H. Li, S. Liu, J. Zhao, N. Feng, Removal of reactive dyes from wastewater assisted with kaolin clay by magnesium hydroxide coagulation process, Colloids Surf. A: Physicochem. Eng. Asp. 494 (2016) 222–227.
[9] L. Yao, L. Zhang, R. Wang, S. Chou, Z. Dong, A new integrated approach for dye removal from wastewater by polyoxometalates functionalized membranes, J. Hazard. Mater. 301 (2016) 462–470.
[10] D.C. de Moura, M.A. Quiroz, D.R. da Silva, R. Saiazar, C.A. Martinez-Huitle, Electrochemical degradation of acid blue 113 dye using TiO_2-nanotubes decorated with PbO_2 as anode, Environ. Nanotechnol. Monit. Manag. 5 (2016) 13–20.
[11] Y. Wang, J. Wang, B. Du, Y. Wang, Y. Xiong, Y. Yang, X. Zhang, Synthesis of hierarchically porous perovskite-carbon aerogel composite catalysts for the rapid degradation of fuchsin basic under microwave irradiation and an insight into probable catalytic mechanism, Appl. Surf. Sci. 439 (2018) 475–487.
[12] W. Astuti, T. Sulistyaningsih, M. Maksiola, Chemically modified kapok sawdust as adsorbent of methyl violet dye from aqueous solution, J. Teknol. (Sci. Eng.) 78 (9) (2016) 367–372.
[13] W. Astuti, T. Sulistyaningsih, M. Maksiola, Equilibrium and kinetics of adsorption of methyl violet from aqueous solutions using modified *Ceiba pentandra* sawdust, Asian J. Chem. 29 (1) (2017) 133–138.
[14] Y. Gao, S. Xu, Q. Yue, Y. Wu, B. Gao, Chemical preparation of crab shell based activated carbon with superior adsorption performance for dye removal from wastewater, J. Taiwan Inst. Chem. Eng. 61 (2016) 327–335.
[15] J.E. Aguiar, J.C.A. de Oliveira, P.F.G. Silvino, J.A. Neto, I.J. Silva Jr., S.M.P. Lucena, Correlation between PSD and adsorption of anionic dyes with different molecular weight on activated carbon, Colloids Surf. A: Physicochem. Eng. Asp. 496 (2016) 125–131.
[16] M.J. Ahmed, Application of agricultural based activated carbon by microwave and conventional activations for basic dye adsorption: review, J. Environ. Chem. Eng. 4 (1) (2016) 89–99.
[17] J. Li, D.H.L. Ng, P. Song, C. Kong, Y. Song, Synthesis of SnO_2-activated carbon fiber hybrid catalyst for the removal of methyl violet from water, Mater. Sci. Eng. B 194 (2015) 1–8.
[18] A.M. Herera-González, M. Caldera-Villalobos, A. Peláez-Cid, Adsorption of textile dyes using an activated carbon and crosslinked polyvinyl phosphonic acid composite, J. Environ. Manag. 234 (2019) 237–244.
[19] A.F.M. Streit, L.N. Côrtes, S.P. Druzian, M. Godinho, G.L. Dotto, Development of high quality activated carbon from biological sludge and its application for dyes removal from aqueous solutions, Sci. Total Environ. 660 (2019) 277–287.
[20] X. Zhang, Y. Yang, X. Lv, Y. Wang, N. Liu, D. Chen, L. Cui, Adsorption/desorption kinetics and breakthrough of gaseous toluene for modified micro-porous–mesoporous UiO-66 metal organic framework, J. Hazard. Mater. 366 (2019) 140–150.
[21] X. Zhang, X. Lv, X. Shi, Y. Yang, Y. Yang, Enhanced hydrophobic UiO-66 (University of Oslo 66) metal-organic framework with high capacity and selectivity for toluene capture from high humid air, J. Colloid Interface Sci. 539 (2019) 152–160.
[22] N. Boudechiche, M. Fares, S. Ouyahia, H. Yazid, M. Trari, Z. Sadaoui, Comparative study on removal of two basic dyes in aqueous medium by adsorption using activated carbon from *Ziziphus lotus* stones, Microchem. J. 146 (2019) 1010–1018.
[23] L. Lin, Y. Lin, C. Li, D. Wu, H. Kong, Synthesis of zeolite/hydrous metal oxide composites from coal fly ash as efficient adsorbents for removal of methylene blue from water, Int. J. Miner. Process. 148 (2016) 32–40.
[24] F. Mushtaq, M. Zahid, I.A. Bhatti, S. Nasir, T. Hussain, Possible applications of coal fly ash in wastewater treatment, J. Environ. Manag. 240 (2019) 27–46.
[25] L. Yang, D. Li, Z. Zhu, M. Xu, X. Yan, H. Zhang, Effect of the intensification of preconditioning on the separation of unburned carbon from coal fly ash, Fuel 242 (2019) 3174–3183.
[26] M.M. Orta, J. Martin, S. Medina-Carrasco, J.L. Santos, I. Aparicio, E. Alonso,

Adsorption of propranolol onto montmorillonite: kinetic, isotherm and pH studies, Appl. Clay Sci. 171 (2019) 107–114.
[27] S. Azizian, S. Eris, L.D. Wilson, Re-evaluation of the century-old Langmuir isotherm for modeling adsorption phenomena in solution, Chem. Phys. 513 (2018) 99–104.
[28] C. Srilakshmi, R. Saraf, Ag-doped hydroxyapatite as efficient adsorbent for removal of Congo red dye from aqueous solution: synthesis, kinetic and equilibrium adsorption isotherm analysis, Microporous Mesoporous Mater. 219 (2016) 134–144.
[29] K.B. Fontana, E.S. Chaves, J.D.S. Sanchez, E.R.L.R. Watanabe, J.M.T.A. Pietrobelli, G.G. Lenzi, Textile dye removal from aqueous solutions by malt bagasse: isotherm, kinetic and thermodynamic studies, Ecotoxicol. Environ. Saf. 124 (2016) 329–336.
[30] A. Hassani, F. Vafaei, S. Karaca, A.R. Khataee, Adsorption of cationic dye from aqueous solution using Turkish lignite: kinetic, isotherm, thermodynamic studies and neural network modeling, J. Ind. Eng. Chem. 20 (2014) 2615–2624.
[31] T.S. Anirudhan, M. Ramachandran, Adsorptive removal of basic dyes from aqueous solutions by surfactant modified bentonite clay (organoclay): kinetic and competitive adsorption isotherm, Process Saf. Environ. Prot. 95 (2015) 215–225.
[32] C. Arora, S. Soni, S. Sahu, J. Mittal, P. Kumar, P.K. Bajpai, Iron based metal organic framework for efficient removal of methylene blue dye from industrial waste, J. Mol. Liq. 284 (2019) 343–352.
[33] M.T. Islam, F. Aimone, A. Ferri, G. Rovero, Use of N-methylformanilide as swelling agent for meta-aramid fibers dyeing: kinetics and equilibrium adsorption of basic blue 41, Dyes Pigments 113 (2015) 5554–5561.
[34] W. Astuti, A. Prasetya, E.T. Wahyuni, I.M. Bendiyasa, The effect of unburned carbon on coal fly ash toward its adsorption capacity for methyl violet, Int. J. Chem. Mol. Eng. 7 (6) (2013) 418–421.
[35] L. Yan, L. Qin, H. Yu, S. Li, R. Shan, B. Du, Adsorption of acid dyes from aqueous solution by CTMAB modified bentonite: kinetic and isotherm modeling, J. Mol. Liq. 211 (2015) 1074–1081.
[36] W. Astuti, I.M. Bendiyasa, E.T. Wahyuni, A. Prasetya, The effect of coal fly ash crystallinity toward methyl violet adsorption capacity, AJChE 10 (1) (2010) 8–14.
[37] P. Rai, R.K. Gautam, S. Banerjee, V. Rawat, M.C. Chattopadhyaya, Synthesis and characterization of a novel $SnFe_2O_4$@activated carbon magnetic nanocomposite and its effectiveness in the removal of crystal violet from aqueous solution, J. Environ. Chem. Eng. 3 (4 (Pt A)) (2015) 2281–2291.